J. Fluid Mech. (1967), *vol.* 29, *part* 4, *pp.* 765–779
Printed in Great Britain

Shock curvature and gradients at the tip of pointed axisymmetric bodies in non-equilibrium flow

By RAYMOND SEDNEY† AND NATHAN GERBER
Ballistic Research Laboratories, Aberdeen Proving Ground, Md.

(Received 19 December 1966)

The shock curvature and flow variable gradients at the tip of a pointed body caused by non-equilibrium effects are considered. Co-ordinates introduced by Chester (1956) are used since they offer a convenient way of treating the boundary conditions. The desired functions are obtained by solving numerically a system of linear ordinary differential equations. These equations have a singularity; the nature of the singularity is found analytically, and its numerical treatment is discussed. The specific non-equilibrium effect considered is vibrational relaxation in a pure diatomic gas. Representative results are given for flow of N_2 over a cone for a comprehensive range of Mach number and cone angle. There is a point analogous to the Crocco point. The exact results are compared with predictions from (i) a hypersonic, small disturbance theory; (ii) the application of an integral method; (iii) characteristic calculations. In an appendix, a comparative discussion is given of results for frozen flow over ogival bodies.

1. Introduction

When non-equilibrium effects are considered in the fluid dynamic equations, the classical similar solutions describing supersonic flow over wedges and cones no longer exist. To gain some insight into non-equilibrium effects one can seek solutions valid in restricted regions of a flow, e.g. the vicinity of the tip of a wedge or cone. The first approximation to the flow here is the frozen (similar) solution. The next approximation brings into evidence the non-equilibrium effects, such as the curvature of the shock wave. The purpose of this work is to find this approximation for the case of flow over a cone and pointed ogives in general.

The corresponding problem for wedge flow (Sedney 1961) is resolved by explicit solution of algebraic equations. For cone flow, differential equations with two-point boundary conditions (at shock and body surfaces) must be solved. The coefficients of these equations which involve the frozen conical flow solution, give rise to a singular point at least in all choices of co-ordinates investigated.

There is a close analogy between the problem of approximating the non-equilibrium flow in the neighbourhood of the tip of a wedge or cone and that of approximating the equilibrium or frozen flow near the tip of a pointed ogive body. The latter problem was solved by Crocco (1937) for two-dimensional flow

† Present address: R.I.A.S., 1450 S. Rolling Road, Baltimore, Maryland 21227.

and by Shen & Lin (1951) for axisymmetric flow. In order to treat the singularity for the axisymmetric case, and especially its effects on higher approximations, Kogan (1956) formulated the problem in terms of Crocco's stream function. This refinement, however, is not included in the values of shock curvature hitherto published (Shen & Lin 1951; Bianco, Cabannes & Kuntzmann 1960). In the method of solution adopted here for determining shock curvature and gradients caused by non-equilibrium effects, these same quantities for frozen flow over ogival bodies are obtained as a by-product. Significant differences were obtained between the present results and those of Shen & Lin (1951) and Bianco *et al.* (1960). This is discussed in the appendix.

The specific source of the non-equilibrium effects considered here is vibrational relaxation of a diatomic gas; the present method, however, can be employed for dissociation, ionization, etc. The model of a vibrationally excited gas serves as well as any other example to illustrate the technique and effects.

A distinctive feature of this analysis is the choice of co-ordinates. Specifically the co-ordinates used are those introduced by Chester (1956) in his study of hypersonic flow over blunt bodies. The chief advantage of this choice is the ease of handling the boundary conditions on the shock; for here the unknown shock curve is mapped into one of the co-ordinate lines. Also the singular point at the tip is spread out into a line interval along the second co-ordinate axis. The latter advantage is also gained with polar co-ordinates, but not the former. The differential equations now have an integrable, inverse one-half power, type of singularity at the origin. This could be handled in the standard way—using expansions to match the numerical solution; instead the entire problem is treated numerically, the authors believing this procedure to be more efficient. The singularity is treated by a 'detailed approach to the body' which involves decreasing the step size in the Runge–Kutta numerical integration procedure.

One motivation for this work arose in the computation of non-equilibrium flows over cones (Sedney & Gerber 1963) by the method of characteristics. That calculation was initiated by assuming a finite frozen flow region. The effect of this error can be relatively large and propagate two or three lengths of the original frozen region even though the grid size is twenty to thirty times less than this length. The behaviour near the tip was studied by the laborious process of choosing successively smaller frozen flow regions; the method presented here is more satisfactory for obvious reasons. The results of the present paper can be used as a check on those from the characteristic method. Alternatively, they can be used as input to start the characteristics calculation. With the improved approximation to the flow near the tip, a larger grid size is possible and a saving on computation time realized.

Having the exact results allows comparisons to be made with various approximate methods; this is done in § 6.

2. Flow equations

The axisymmetric flows to be considered are steady, inviscid and isoenergetic. The equations for conservation of mass, momentum, and energy are, in *non-dimensional form*,

$$\frac{\partial}{\partial x}(y\rho u)+\frac{\partial}{\partial y}(y\rho v)=0, \tag{2.1}$$

$$\gamma \mathrm{M}_\infty^2\left[u\frac{\partial u}{\partial x}+v\frac{\partial u}{\partial y}\right]=-\frac{1}{\rho}\frac{\partial p}{\partial x}, \tag{2.2}$$

$$\gamma \mathrm{M}_\infty^2\left[u\frac{\partial v}{\partial x}+v\frac{\partial v}{\partial y}\right]=-\frac{1}{\rho}\frac{\partial p}{\partial y}, \tag{2.3}$$

$$\tfrac{1}{2}(\gamma-1)M_\infty^2(u^2+v^2)+T+E=h_t. \tag{2.4}$$

See figure 1 for notation (where primes indicate dimensional quantities); ρ is density, p is pressure, T is temperature, E is vibrational energy per unit mass, γ is the ratio of frozen specific heats, and h_t is the constant total enthalpy. Variables are made dimensionless as follows: lengths by $\tau_b' q_\infty'$, where τ_b' is the relaxation

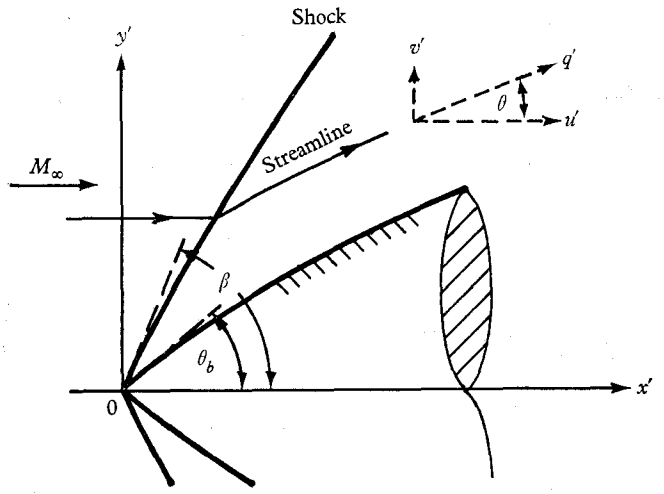

FIGURE 1. Cross-sectional view of flow field in the physical plane. (q' = flow speed; u', v' = velocity components in co-ordinate directions.)

time evaluated at the frozen conditions on the body tip and q_∞' is free-stream velocity; velocities, pressure, density and temperature by their free-stream values; vibrational energy by $c_{pa}'T_\infty'$, the frozen enthalpy in the free stream. The model chosen for the diatomic gas with vibrational relaxation is discussed in Sedney (1961). The perfect gas law is assumed

$$p=\rho T \tag{2.5}$$

and the rate equation is

$$u\frac{\partial E}{\partial x}+v\frac{\partial E}{\partial y}=[E^*(T)-E]/\tau\equiv\Phi, \tag{2.6}$$

where τ is the relaxation time referred to τ_b', and $E^*(T)$ is the local equilibrium value of E, given by

$$E^*(T)=(\tfrac{2}{7}Z)/(e^{Z/T}-1)$$

with $Z = \Theta_v'/T_\infty'$, Θ_v' = characteristic vibrational temperature. The variation of τ with T and p is approximated by

$$\tau = (p_b/p)\exp\left[(c/T)^{\frac{1}{3}} - (c/T_b)^{\frac{1}{3}}\right]$$

and the subscript b refers to conditions on the body at the tip. The constant c is evaluated for various temperature ranges by fitting experimental data; e.g. those of Blackman (1956) or Millikan & White (1963).

The independent variables x, y are transformed to ζ, η by

$$\zeta = 2\psi(x,y)/y^2, \quad \eta = y, \tag{2.7}$$

where ψ is the dimensionless streamfunction

$$\partial\psi/\partial x = -y\rho v, \quad \partial\psi/\partial y = y\rho u.$$

Thus $$\frac{\partial}{\partial x} = -\frac{2\rho v}{\eta}\frac{\partial}{\partial\zeta} \quad \text{and} \quad \frac{\partial}{\partial y} = \frac{\partial}{\partial\eta} + \frac{2(\rho u - \zeta)}{\eta}\frac{\partial}{\partial\zeta};$$

and equations (2.1), (2.2), (2.3) and (2.6) become, respectively,

$$2\frac{\partial}{\partial\zeta}\left(\frac{u}{v}\right) - 2\frac{\partial}{\partial\zeta}\left(\frac{\zeta}{\rho v}\right) + \frac{\partial}{\partial\eta}\left(\frac{\eta}{\rho v}\right) = 0, \tag{2.8}$$

$$\left(\frac{2}{\gamma M_\infty^2}\right)\frac{\partial p}{\partial\zeta} = \eta\frac{\partial u}{\partial\eta} - 2\zeta\frac{\partial u}{\partial\zeta}, \tag{2.9}$$

$$\left(\frac{\gamma M_\infty^2}{2}\right)\left[\eta\frac{\partial}{\partial\eta}(u^2+v^2) - 2\zeta\frac{\partial}{\partial\zeta}(u^2+v^2)\right] = -\frac{1}{\rho}\left(\eta\frac{\partial p}{\partial\eta} - 2\zeta\frac{\partial p}{\partial\zeta}\right), \tag{2.10}$$

$$v\left(\eta\frac{\partial E}{\partial\eta} - 2\zeta\frac{\partial E}{\partial\zeta}\right) = \frac{\eta}{\tau}[E^*(T) - E]. \tag{2.11}$$

Note that if vibrational energy in the free stream is negligible ($E_\infty = 0$)

$$h_t = 1 + \tfrac{1}{2}(\gamma - 1)M_\infty^2.$$

This would be the case if $T_\infty \ll \Theta_v$ and equilibrium existed in the free stream. If the free stream is out of equilibrium E_∞ will, in general, not be negligible. This would occur, e.g., if a cone were placed in the test section of a shock tunnel, since the free stream is generally frozen in such a facility. In any case, behind the shock E takes its free-stream value.

The variables ζ and η were employed by Chester in the study of hypersonic flow past blunt bodies. In the present problem the shock wave is attached at the pointed tip of the body, but the flow region is mapped into the same strip of the (ζ, η)-plane as for the case of a detached shock. This strip is shown in figure 2, where it is seen that the tip transforms into the line segment $\eta = 0$, $0 \leqslant \zeta \leqslant 1$. This stretching is necessary to examine the singularity at the tip. It is also accomplished by using polar co-ordinates (when properly plotted on rectangular axes); however, the shock curve is unknown then. The same strip is obtained if a body-oriented co-ordinate system is used and the normal co-ordinate is normalized by the total distance between the body and the shock.

If the body is a cone and the flow is either frozen or in equilibrium so that the flow is conical, then the flow variables are constant along the lines $\zeta =$ constant. This is shown by using the fact that ψ is homogeneous of degree two in the variables x and y, a result which follows from the definition of ψ and the fact that ρu and ρv are homogeneous of degree zero. The streamlines are always the hyperbolae, $\zeta\eta^2 =$ constant.

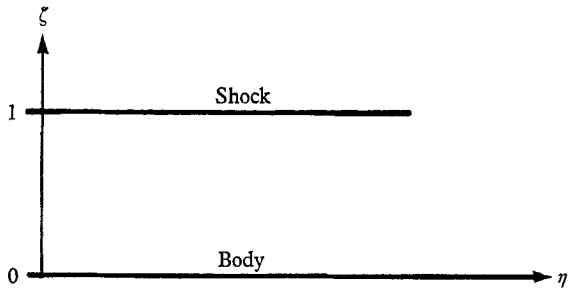

FIGURE 2. Flow region in the (ζ, η)-plane.

On physical grounds one would expect that the flow at the tip, $\eta = 0$, should be frozen; this is easily proved from (2.8)–(2.11). Setting $\eta = 0$, all terms containing $\partial/\partial\eta$ vanish, $\partial E/\partial\zeta = 0$, and the remaining equations give

$$\left.\begin{aligned} \frac{du}{d\zeta} &= \frac{1}{2}\left(\frac{pv}{\rho^2}\right)/D, \\ \frac{dv}{d\zeta} &= -\frac{1}{2}\left[\frac{p(\rho u-\zeta)}{\rho^3}\right]/D, \\ \frac{d\rho}{d\zeta} &= -\frac{1}{2}\left(\frac{M_\infty^2\zeta v}{\rho}\right)/D, \\ \frac{dp}{d\zeta} &= -\frac{1}{2}\left(\frac{\gamma M_\infty^2 pv\zeta}{\rho^2}\right)/D, \end{aligned}\right\} \tag{2.12}$$

where

$$D = \frac{p(\rho u-\zeta)^2}{v\rho^3} + \frac{v}{\rho}\left(p - \frac{M_\infty^2\zeta^2}{\rho}\right). \tag{2.13}$$

Since $\partial E/\partial\zeta = 0$ along $\eta = 0$, E is then constant there; i.e. the flow is frozen at the tip. The constant will be the free-stream value of E.

The equations (2.12) are those for conical frozen (Taylor–Maccoll) flow in the co-ordinates ζ, η; their numerical solution is a necessary step in the determination of the gradients since the frozen flow variables appear as coefficients in the gradient equations. This solution is obtained by integrating from the shock, $\zeta = 1$, to the body, $\zeta = 0$, given M_∞, γ and β, where $\tan\beta$ is the shock wave slope. The initial conditions at the shock are the standard frozen shock relations:

$$u_w = 1 - \frac{2(M_\infty^2\sin^2\beta - 1)}{(\gamma+1)M_\infty^2}, \tag{2.14}$$

and so forth. The half-angle of the body tip is determined from

$$\tan\theta_b = (v/u)_{\zeta=0}. \tag{2.15}$$

One can integrate several cases and then interpolate to find a desired half-angle or set up an iteration procedure to yield this result.

3. Gradient equations

The equations for the gradients of the flow variables are obtained by differentiating (2.8)–(2.11) with respect to η, then setting η equal to zero. This requires the assumption† that $\partial^2/\partial\zeta\partial\eta = \partial^2/\partial\eta\partial\zeta$.

The following notation is introduced:

$$\left.\begin{aligned} U &= (\partial u/\partial\eta)_{\eta=0}, \quad V = (\partial v/\partial\eta)_{\eta=0}, \quad \Omega = (\partial E/\partial\eta)_{\eta=0}, \\ R &= (\partial\rho/\partial\eta)_{\eta=0}, \quad P = (\partial p/\partial\eta)_{\eta=0}. \end{aligned}\right\} \tag{3.1}$$

Hereafter, it is to be understood that all quantities are evaluated at $\eta = 0$. The differential equations for the gradient functions are (where $\cdot \equiv d/d\zeta$)

$$\dot{\Omega} = (\Omega - \Phi/v)/(2\zeta), \tag{3.2}$$

$$\dot{U} = (1/D)\,[vG/\rho + b(C - \epsilon\Omega)/\zeta], \tag{3.3a}$$

$$\dot{V} = (1/D)\,[-gG/\rho + f(C - \epsilon\Omega)/\zeta], \tag{3.3b}$$

$$\dot{R} = -[M_\infty^2 v\zeta B + (g^2 + v^2)\,(A - \epsilon F)/v + j(C - \epsilon\Omega)/\zeta]/D, \tag{3.3c}$$

where the denominator D is the same as in (2.13).

The coefficients g, b, f and j are known functions of ζ:

$$\left.\begin{aligned} g &= u - \zeta/\rho, \\ b &= [pg/v - (\gamma - 1)\,M_\infty^2 v\zeta]/(2\gamma M_\infty^2\rho), \\ f &= [\zeta M_\infty^2(\gamma g - u) + p]/(2\gamma M_\infty^2\rho), \\ j &= \rho[(\gamma - 1)\,v^2 + g(\gamma g - u)]/(2\gamma v), \end{aligned}\right\} \tag{3.4}$$

where u, v, ρ and p have been obtained from the solution to (2.12); Φ is given in (2.6). The symbol ϵ is equal to zero for frozen flow (no vibrational relaxation), and one for non-equilibrium flow.

The coefficients A, B, C, F and G are linear functions of U, V, R and Ω:

$$\left.\begin{aligned} A &= -M_\infty^2[\gamma/2 + (\gamma - 1)\,(u\dot{\rho} + \rho\dot{u})]\,U - (\gamma - 1)\,M_\infty^2(v\dot{\rho} + \rho\dot{v})\,V \\ &\quad + (\gamma - 1)\,(p\dot{\rho}/\rho^2)\,R, \\ B &= (\dot{v}/v)\,U + [\dot{u}/v + (\zeta\dot{\rho})/(\rho^2 v) - 2\dot{v}g/v^2]\,V \\ &\quad + (\zeta/\rho^2)\,(\dot{v}/v + 2\dot{\rho}/\rho)\,R, \\ C &= M_\infty^2(u - 2\gamma\zeta\dot{u} - \gamma\zeta/\rho)\,U + M_\infty^2(v - 2\gamma\zeta\dot{v})\,V \\ &\quad + (1/\rho^2)\,(p + 2\zeta\dot{p})\,R, \\ F &= \dot{\rho}\Omega + (1/\zeta)\,(\rho/2)\,(\Omega - \Phi/v), \\ G &= pB + \zeta A/\rho - \epsilon[\zeta\dot{\rho}\Omega/\rho + \tfrac{1}{2}(\Omega - \Phi/v)]. \end{aligned}\right\} \tag{3.5}$$

† The set of mathematical conditions ensuring the interchangeability of second derivatives is different from that ensuring the validity of an expansion of the form

$$f(\eta, \zeta)_b + (\partial f/\partial\eta)_b\,\eta + O(\eta^2).$$

Neither set can be verified *a priori*.

Equation (3.2) can be solved separately, using the initial condition,

$$\Omega(\zeta = 1) = 0$$

(since E does not change along $\zeta = 1$); then Ω can be treated as a known function of ζ in (3.3). Equations (3.3) are linear equations in U, V and R, homogeneous when $\epsilon = 0$ and non-homogeneous when $\epsilon = 1$.

The pressure gradient function P_b is obtained by differentiating (2.10) with respect to η and taking $\eta = \zeta = 0$:

$$P_b = -\gamma M_\infty^2 \rho_b (uU + vV)_b. \tag{3.6}$$

Initial conditions are applied at the shock wave, $\zeta = 1$; conditions there will be designated by the subscript w. For any function f

$$\partial f/\partial \eta]_{\zeta=1} = (\csc\beta)\, df/d\sigma = (\csc\beta)\,(df/d\beta)\, K_w,$$

where σ is arc length along the shock wave and $K_w \equiv d\beta/d\sigma$ is the curvature of the shock. The initial conditions are

$$\left.\begin{aligned} U_w &= (du/d\beta)\, K_w \csc\beta, \quad V_w = (dv/d\beta)\, K_w \csc\beta, \\ R_w &= (d\rho/d\beta)\, K_w \csc\beta, \end{aligned}\right\} \tag{3.7}$$

where $du/d\beta$, $dv/d\beta$ and $d\rho/d\beta$ are obtained by differentiating the shock relations; e.g. (2.14).

The solution to equations (3.3) can be written

$$U = K_w U_h + U_n, \quad V = K_w V_h + V_n, \quad R = K_w R_h + R_n, \tag{3.8}$$

where U_h, V_h and R_h are the solutions to the homogeneous equations satisfying the initial conditions (3.7) with $K_w = 1$; U_n, V_n and R_n are particular solutions to the non-homogeneous equations satisfying the initial conditions

$$(U_n)_w = (V_n)_w = (R_n)_w = 0.$$

With the solutions $U_h, U_n, \ldots, R_n$ determined it remains to find K_w for the complete solution (3.8). This is found by applying the terminal condition (2.15) to the gradient functions. From equation (2.15) one obtains

$$V_b = U_b \tan\theta_b + u_b \sec^2\theta_b (\partial\theta_b/\partial\eta)_{\eta=0}, \tag{3.9}$$

also

$$(\partial\theta_b/\partial\eta)_{\eta=0} = K_b \csc\theta_b, \tag{3.10}$$

where $K_b \equiv d\theta_b/ds$ denotes the curvature of the body at the tip, and s the arc length along the body. Combining (3.8), (3.9) and (3.10) gives the shock curvature in terms of the body curvature

$$K_w = \left[\frac{u\sec^2\theta\csc\theta}{V_h - U_h\tan\theta}\right]_b K_b - \left[\frac{V_n - U_n\tan\theta}{V_h - U_h\tan\theta}\right]_b. \tag{3.11}$$

Finally, the gradients on the body are given by

$$\left.\begin{aligned} (dp/ds)_b &= P_b \sin\theta_b, \quad (dE/ds)_b = \Omega_b \sin\theta_b, \\ (dT/ds)_b = (\rho P - pR)_b (\sin\theta_b)/\rho_b^2, &\quad (dq/ds)_b = (uU + vV)_b (\sin\theta_b)/q_b, \end{aligned}\right\} \tag{3.12}$$

where P is given by (3.6).

Equation (3.11) shows that the shock wave curvature at the tip of a pointed body of revolution is the sum of two terms: (i) the curvature for a curved body in frozen flow, and (ii) the curvature for non-equilibrium flow over a cone.

Previous calculations (Shen & Lin 1951; Bianco *et al.* 1960) have been made of K_b/K_w for ideal gas flows ($\epsilon = 0$ in equations (3.3), see appendix). These and calculations from the present work indicate that K_b/K_w becomes zero for every axisymmetric body at some M_∞ which produces a partially subsonic, partially supersonic conical flow at the tip ($\eta = 0$). This implies that, for each θ_b, there is an M_∞ for which, according to (3.11),

$$(V_h - U_h \tan\theta)_b = 0.$$

This is the 'Crocco point' in axisymmetric flow (see, e.g., Ferri 1954). It is also seen, from (3.11), that for these same values of M_∞ and θ_b the curvature of the shock wave in non-equilibrium flow becomes infinite at the tip of the cone (where $K_b = 0$).

4. Solution in the vicinity of the singular point

The equations for the gradient functions (3.2) and (3.3) have a regular singular point at $\zeta = 0$. Following Ince (1926) the first step in examining the nature of the solutions in the neighbourhood of the singular point is to set up the indicial equation and find its roots. When this is done for (3.2) and (3.3) it is found that the roots are: $0, 0, \frac{1}{2}, \frac{1}{2}$. The presence of the two double roots indicates that logarithmic terms must be included. Thus, each variable has the form

$$P_1 + (\log\zeta)\, P_2 + \zeta^{\frac{1}{2}} P_3 + (\zeta^{\frac{1}{2}} \log\zeta)\, P_4, \tag{4.1}$$

where the P_i denote power series with unknown coefficients. Recurrence relations obtained by substituting these forms into the differential equations determine the coefficients of the power series in terms of the arbitrary constants.

Since a numerical solution to equations (3.2) and (3.3) is obtained, a lengthy discussion of the singularity is not needed. Suffice it to say that the constant terms in the series P_2 and P_4 are zero for each variable. Thus, each gradient function has the form

$$\text{constant} + (\zeta^{\frac{1}{2}} \times \text{constant}) \tag{4.2}$$

in the neighbourhood of $\zeta = 0$.

5. Numerical solution

Equations (2.12) are first solved separately; then (3.2) and (3.3) are solved. The Runge–Kutta–Gill method is used to integrate the equations numerically.

With high-speed computers it is possible to study the solution empirically by carrying out a 'detailed approach' to the body; that is, to systematically decrease the interval size in the Runge–Kutta–Gill procedure as ζ approaches zero, ending the calculation at an extremely small but finite value of $\zeta (\sim 10^{-12})$. This is the method used in the present work. While admittedly not elegant, this procedure does produce answers in reasonably short times, and *a posteriori* tests indicate that the values obtained are correct. Thus, unique limits for the gradient functions are found as the integration interval and limiting ζ approach

zero; also, the calculated gradient functions exhibit the $\zeta^{\frac{1}{2}}$ variation near zero, (4.2), which was demonstrated in §4. In addition, the calculated solution to (3.2) agrees with the known value ($\Omega = \Phi/v$) obtained from Taylor–Maccoll flow.

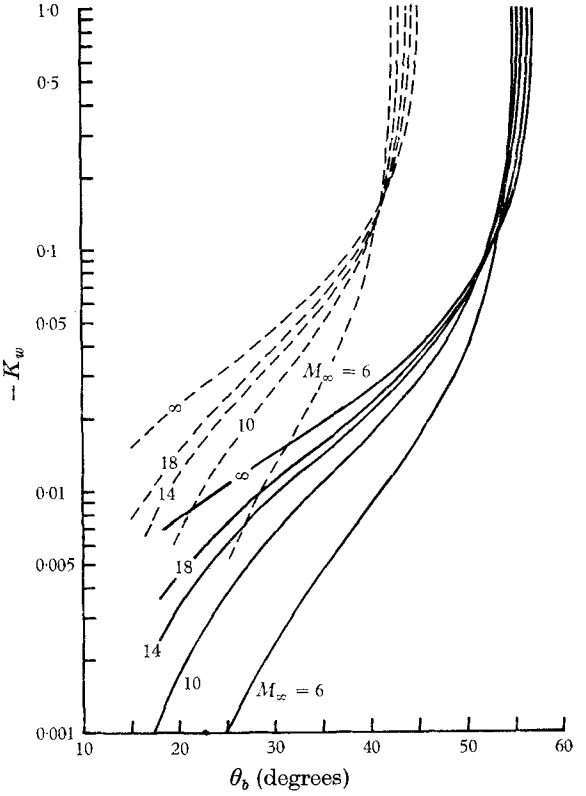

FIGURE 3. Shock wave curvature at the tip of pointed body *vs.* body half-angle; N_2 gas, $T'_\infty = 300$ °K. Solid lines refer to cones, dotted lines to wedges.

6. Results

In the case of cones (where $K_b = 0$) the shock curvature K_w reduces to the second term of the expression in (3.11). This quantity was calculated for a wide range of Mach numbers and cone angles for nitrogen at 300 °K. Results are shown in figure 3 (solid curves). Each curve has a vertical asymptote occurring at a cone angle for which the Taylor–Maccoll flow is supersonic at the shock wave, but subsonic at the body; K_w changes sign here and then decreases in absolute value with increasing θ_b. The qualitative behaviour of K_w is similar to that of shock curvature at a wedge tip, shown also in figure 3. Figure 4 shows the variation of the pressure gradient at the tip of a cone; the 'Crocco point' asymptotes appear here also.

From results of Millikan & White (1963) some representative values of $\tau'_b q'_\infty$, the normalizing quantity for distances, are: $\tau'_b q'_\infty = 5{\cdot}2$, 0·26 and 0·034 cm for $\theta_b = 30°$, 40° and 50°, respectively, at $M_\infty = 10$, $p'_\infty = 1$ atmosphere; for other p'_∞, the given $\tau'_b q'_\infty$ is to be divided by the number of atmospheres.

In figure 5 the gradients of pressure, temperature, and density at the tip of a cone are given as functions of cone angle for $M_\infty = 10$, $T'_\infty = 300$ °K in nitrogen. The density gradient is unusual in that it is non-monotonic and changes sign; this change in sign takes place when the flow on the cone surface is subsonic.

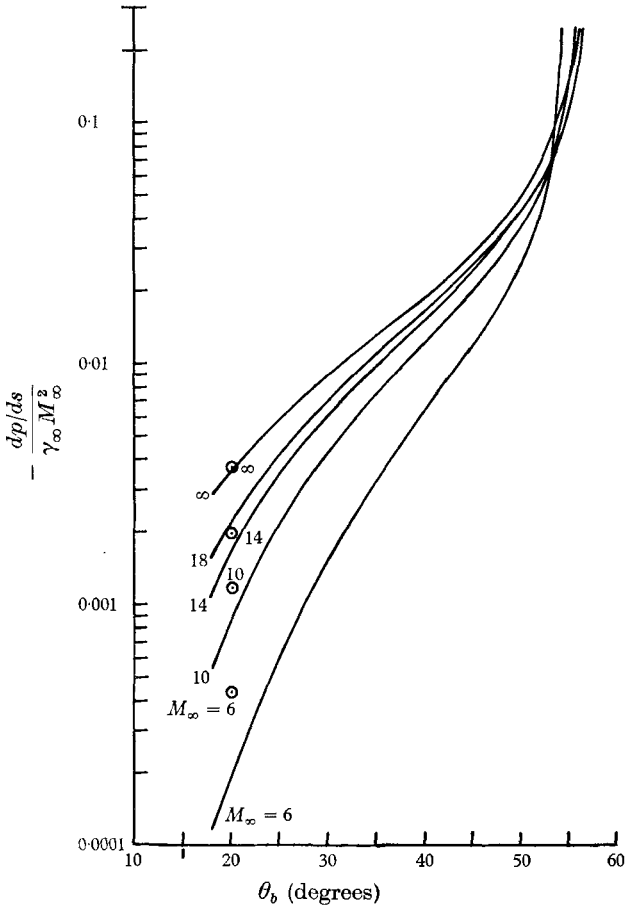

FIGURE 4. Pressure gradient along body at tip of cone *vs.* cone half-angle; N_2 gas, $T'_\infty = 300$ °K. Circled dots: hypersonic small disturbance theory (Lee 1965).

A similar type variation is found for density gradient at the tip of a wedge and is indicated in this figure ; here the change in sign occurs for supersonic flow at the wedge surface. Similar behaviour for the density gradient in plane flow was found for the case of dissociating air,† using the gas model and gradient formulae of Spurk, Gerber & Sedney (1966).

As mentioned in §1, the present work has application in the calculation of axisymmetric non-equilibrium flows. In previous work (Sedney & Gerber 1963), an initial region of frozen flow was assumed in order to start a non-equilibrium

† A characteristic calculation of one example with an initially negative density gradient was performed. The gradient changed sign at a distance of 3 × (initial frozen length) and thereafter was positive. All other flow variables were monotonic.

flow computation by the method of characteristics. This leads to results illustrated in figure 6 for pressure variation on the body in a typical case of flow over a cone. The results are clearly in error near the tip; however, a curve drawn through

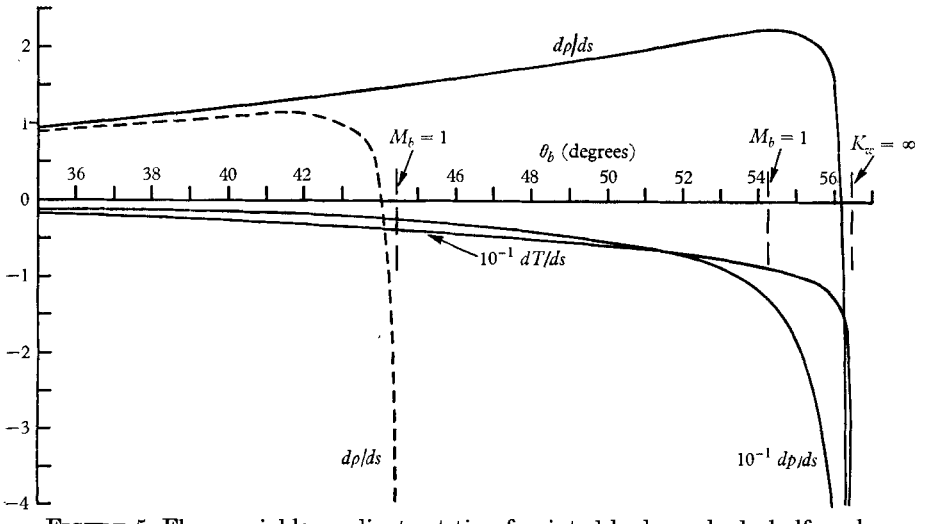

FIGURE 5. Flow variable gradients at tip of pointed body *vs.* body half-angle; N_2 gas, $T'_\infty = 300$ °K, $M_\infty = 10$. Solid lines refer to cone, dotted line to wedge.

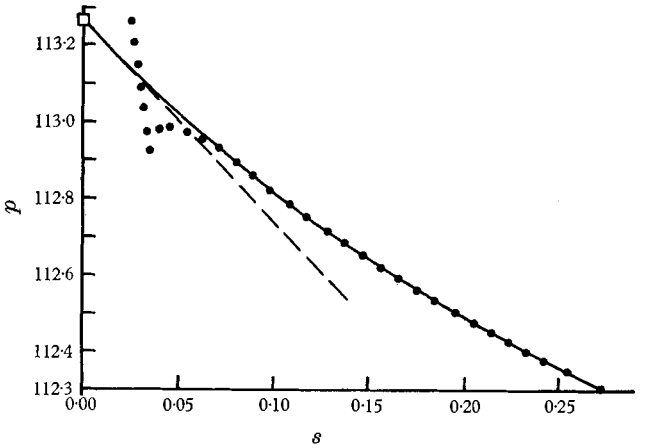

FIGURE 6. Application of pressure gradient calculations to check characteristic calculations; N_2 gas, $T'_\infty = 300$ °K, $M_\infty = 12$, $\theta_b = 46{\cdot}4°$. The dots are characteristic calculation results; the slope of the dashed line is the pressure gradient computed here. □, exact pressure at tip.

the points further downstream can be faired back easily to the correct pressure at the tip, as evidenced by the solid curve. This furnishes an indication that the results downstream are correct. The gradient calculations, indicated by the dashed lines, give further assurance of the validity of the characteristic computations downstream by demonstrating that the solid curve can be extended back to the tip pressure *with the correct slope*. Gradient values can also be useful in initiating non-equilibrium characteristic flow computations.

The present results can be compared with those obtained by an application of Dorodnitsyn's integral method (South & Newman 1965). This latter procedure is an approximate method which yields algebraic equations for the curvature and gradients at the tip of a cone. Figure 7 shows the comparison for two Mach numbers. The agreement, in general, is good; it is found to improve as the angle interval $\beta - \theta_b$ decreases.

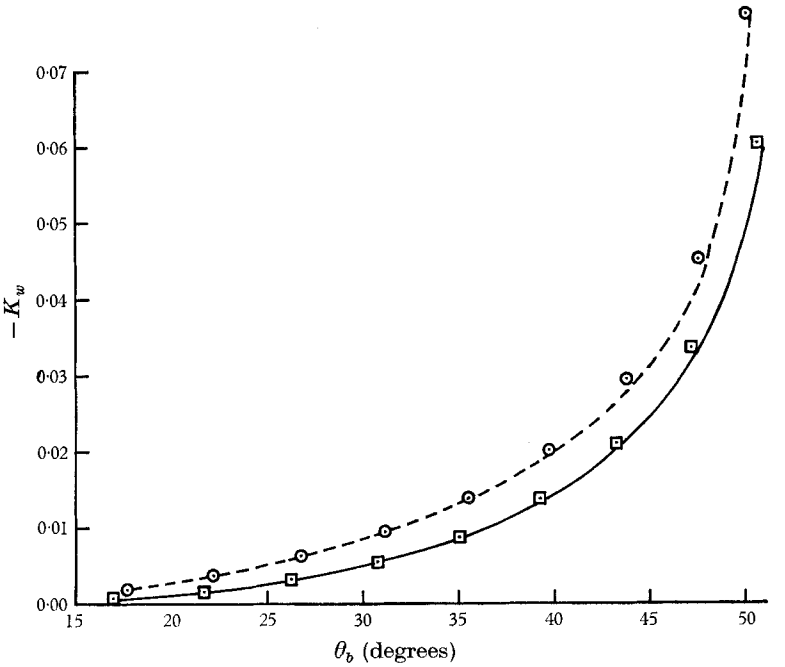

FIGURE 7. Comparison of present calculations of shock wave curvature with integral method calculations of South & Newman; N_2 gas, $T'_\infty = 300$ °K. The lines represent results of present computations: solid line, $M_\infty = 8$; dashed line, $M_\infty = 12$. The dots represent results of South & Newman: ⊡, $M_\infty = 8$; ⊙, $M_\infty = 12$.

An interesting comparison can be made between these exact results and the predictions from the theory of hypersonic flow over slender bodies (Lee 1965). Applying the hypersonic small disturbance approximation results in equations 'too complicated to be integrated analytically', Lee then introduces an additional expansion in the parameter $(\gamma-1)/(\gamma+1)$ and carries this to three terms. The pressure gradient at the tip of a cone was evaluated from this third approximation; the results for $\theta_b = 20°$ are shown in figure 4. Rather large M_∞ are required to have small differences. In the comparison given by Van Dyke (1954) of hypersonic small disturbance theory with exact results for an ideal gas, $M_\infty = 6$ gives small differences. This behaviour is presumably caused by the introduction of the Newtonian type of approximation. Lee illustrates his results for $M_\infty = 15$, $\theta_b = 20°$ and shows agreement with exact calculation to within 2 % for pressure. The present comparison shows that the pressure gradient is 16 % larger than the exact result; this would explain the relatively abrupt overexpansion shown in Lee's results.

7. Conclusion

A method is given for determining the shock curvature and flow variable gradients at the tip of a pointed body of revolution. The use of variables introduced by Chester simplifies setting up the calculations as compared with use of polar co-ordinates. Although the specific source of departure from equilibrium considered here is vibrational excitation, the same technique can be applied to a dissociating gas, with the same qualitative results expected.

It is shown that the shock curvature at the tip of a pointed body of revolution is the sum of two terms: (i) the curvature for a curved body in frozen flow and (ii) the curvature for non-equilibrium flow over a cone. Also, the Crocco point for non-equilibrium flow occurs at the same Mach number and cone angle combination as for frozen flow.

The authors wish to acknowledge here the programming and computing work of Donald Taylor and the assistance of Joan M. Bartos.

Appendix. Some remarks on the flow of a perfect gas over pointed ogives

As pointed out in the introduction, there is an analogy between the problem considered in this paper and that of the flow in the neighbourhood of the tip of a pointed ogive when the flow is considered as frozen or in equilibrium. Since, in the method of solution for the non-equilibrium flow given above, the flow variable gradients and shock curvature—for an ideal gas—are obtained as part of the whole solution, it is appropriate to compare these results with those previously published. This is especially appropriate since some significant differences were noted.

In the work of Shen & Lin (1951), a spurious logarithmic singularity was found. This was an analytical result and, in an addendum, it was later stated to be not actually present. The amended statement would be analogous to showing that P_2 of (4.1) is identically zero. This point is also discussed by Van Dyke (1954). Since the numerical results were independent of the analysis of the singularity, their validity is not in question. However, the numerical results depend on extrapolation of the solution to the body surface.

Bianco *et al.* (1960) give extensive tables for the ratio of curvatures of shock and body. No mention is made of any singular behaviour; these numerical results were also obtained, presumably, by extrapolation to the body surface. Using a first integral, Cabannes (1962) (see also Cabannes & Stael 1961) rephrases the differential equations so that the singularity occurs only in particular integrals of non-homogeneous equations. No results for, say, curvature ratio were given however.

Only a brief summary of the differences will be given here. For an initial angle $\theta_b = 20°$ and $M_\infty = 1{\cdot}88$ the result for curvature ratio of Shen & Lin is 6 % lower than our results; that of Bianco *et al.* is 18 % lower. For smaller M_∞ the percentage difference is greater and vice versa. In the neighbourhood of the maximum curvature ratio, the results of Bianco *et al.* are lower by a factor of two for $\theta_b = 10°$. The primary reason for the differences is in the care that is taken in the numerical

integration near the body. If the integration in the present method is stopped at small, but not 'small enough', values of ζ low values of curvature ratio are obtained.

The results from the present method are more accurate than those previously published because of the method used in approaching the body, see §5. In addition, the accuracy of the results was checked by using much smaller grid sizes and stopping the calculation at smaller values of ζ. Finally, the method of 'extrapolation to zero grid size' was used as a further check.

Interested readers can obtain detailed numerical results from the authors.

Note added in proof

Dr S. H. Maslen has pointed out to the authors that an integral of the gradient equations can be found. Combining equations (2.2)–(2.4), or directly from the first law of thermodynamics,

$$\frac{DE}{Dt}+\frac{1}{\gamma\rho}\frac{Dp}{Dt}-\frac{p}{\rho^2}\frac{D\rho}{Dt}=0.$$

After forming the gradients an integrable equation for $S=(R/\rho)-(P/\gamma p)$ is obtained which gives

$$\zeta^{-\frac{1}{2}}S=-\int(\rho\Phi/2\zeta^{\frac{3}{2}}pv)\,d\zeta+\text{const.}$$

This and the gradients obtained from (2.4) allow R to be eliminated from (3.3a) and (3.3b). Then it can be shown that there are no log terms in (4.1), the only singularity being now in the non-homogeneous terms. The form (4.2) is thus assured for each gradient. The above integral is analogous to that found by Cabannes & Stael (1961).

REFERENCES

Bianco, E., Cabannes, H. & Kuntzmann, J. 1960 Curvature of attached shock waves in steady axially symmetric flow. *J. Fluid Mech.* **7**, 610–616.

Blackman, V. 1956 Vibrational relaxation in oxygen and nitrogen. *J. Fluid Mech.* **1**, 61.

Cabannes, H. 1962 Calcul des gradients de pression et de température à la pointe d'un corps de révolution. *J. Mécanique* **1**, 141–151.

Cabannes, H. & Stael, C. 1961 Singularities of attached shock waves in steady axially symmetric flow. *J. Fluid Mech.* **10**, 289–296.

Chester, W. 1956 Supersonic flow past a bluff body with a detached shock, part II, axisymmetric body. *J. Fluid Mech.* **1**, 490–496.

Crocco, L. 1937 Singolarità della corrente gassosa iperacustica nell'intorno di una prora a diedro. *L'Aerotecnica*, t. xvii, fasc. 6, 519–534.

Ferri, A. 1954 Article in *High Speed Aerodynamics and Jet Propulsion*, vol. vi (p. 678), W. Sears, editor. Princeton University Press.

Ince, E. L. 1926 *Ordinary differential Equations*. New York: Dover 1944.

Lee, R. S. 1965 Hypersonic non-equilibrium flow over slender bodies. *J. Fluid Mech.* **22**, 417–431.

Kogan, A. 1956 On supersonic rotational flow behind strong shock waves, II. Flow past ogives of revolution. *Tech. Rept. Technion Research and Development Foundation, Ltd, Haifa, Israel.*

MILLIKAN, R. C. & WHITE, D. R. 1963 Vibrational energy exchange between N_2 and CO. The vibrational relaxation of nitrogen. *J. Chem. Phys.* **39**, 98–101.

SEDNEY, R. 1961 Some aspects of nonequilibrium flows. *J. Aerospace Sci.* **28**, 189–197.

SEDNEY, R. & GERBER, N. 1963 Nonequilibrium flow over a cone. *AIAA J.* **1**, 2482–2486.

SHEN, S. F. & LIN, C. C. 1951 On the attached curved shock in front of a sharp-nosed axially symmetrical body placed in a uniform stream. *N.A.C.A. Tech. Note* 2505.

SOUTH, J. C. & NEWMAN, P. A. 1965 Application of the method of integral relations to real-gas flows past pointed bodies. *AIAA J.* **3**, 1645–1652.

SPURK, J. H., GERBER, N. & SEDNEY, R. 1966 Characteristic calculation of flowfields with chemical reactions. *AIAA J.* **4**, 30–37.

VAN DYKE, M. D. 1954 A study of hypersonic small-disturbance theory. *NACA Rept.* no. 1194.